Journal of Dentistry 119 (2022) 104054

Contents lists available at ScienceDirect

Journal of Dentistry

journal homepage: www.elsevier.com/locate/jdent

Lithium disilicate and zirconia reinforced lithium silicate glass-ceramics for CAD/CAM dental restorations: biocompatibility, mechanical and microstructural properties after crystallization

Luan Mavriqi [a,1], Francesco Valente [b,c,1], Giovanna Murmura [b,c], Bruna Sinjari [b,c], Monica Macrì [b], Oriana Trubiani [b,c], Sergio Caputi [b,c], Tonino Traini [b,c,1,*]

[a] Department of Dentistry, Albanian University, Tirana 1001, Albania
[b] Department of Innovative Technologies in Medicine and Dentistry, University "G. d'Annunzio" of Chieti-Pescara, Via dei Vestini 31, Chieti 66100, Italy
[c] Electron Microscopy Laboratory, University "G. d'Annunzio" of Chieti-Pescara, Via dei Vestini 31, Chieti 66100, Italy

ARTICLE INFO

Keywords:
Glass-ceramics
ZLS
Lithium disilicate
Biocompatibility
Crystallization
Differential thermal analysis

ABSTRACT

Objectives: The objective of this study was to define the impact of heating rate on the crystal growth, the mechanical properties, and the biocompatibility of three different kinds of CAD/CAM glass-ceramics treated with a conventional furnace.

Methods: Lithium disilicate (IPS EMax-CAD, Ivoclar Vivadent) (LS_2) and two zirconia reinforced lithium silicate (ZLS) ceramics (Vita Suprinity PC, VITA Zahnfabrik; Celtra Duo, Dentsply Sirona) (ZLSS; ZLSC) were used. The mechanical properties and the crystal growth were evaluated on 42 specimens ($n = 14$ per group). The thermal treatments recommended by the manufacturers were carried out. All groups were tested for fracture toughness (Ft) and Vickers hardness (Hv). Scanning electron microscope (SEM) images were taken after a slight surface etching with hydrofluoric acid solution (1% for 20 s). Differential Thermal Analysis (DTA) was performed and cellular adhesion with human periodontal ligament stem cells (hPDLSCs) culture was qualitatively assayed. Data were analyzed with Repeated Measurements ANOVA and ANOVA followed by Tukey post hoc test.

Results: The crystals' mean size (±SD) after heat treatment was 1650.0 (±340.0) nm for LS_2, 854.5 (±155.0) nm for ZLSS and 759.9 (±118.4) nm for ZLSC ($p < 0.05$ among the groups). As consequence of crystallization, the Hv was 6.1 ± 0.3 GPa for LS_2, 7.6 ± 0.7 GPa for ZLSS and 7.1 ± 0.5 GPa for ZLSC ($p < 0.05$ for LS_2 vs ZLSS and ZLSC), while the Ft was 2.2 ± 0.1 MPa $m^{1/2}$ for LS_2, 4.7 ± 0.8 MPa $m^{1/2}$ for ZLSS and 3.8 ± 0.6 MPa $m^{1/2}$ for ZLSC ($p < 0.05$ among the groups). The DTA curves showed a crystallization process for LS_2, ZLSS and ZLSC at a temperature range 810–840 °C. The amount of adherent hPDLSCs was superior on LS_2 than on ZLS.

Conclusions: All the CAD/CAM materials can be properly crystallized if heat treated following the manufacturers' instructions. The crystallization process highly depends on temperature. ZLS glass ceramics show significantly inferior crystals dimensions and higher fracture toughness and Vickers hardness than LS_2 ceramic. hPDLSCs cultured on LS_2 have a superior adhesion than those cultured on ZLS.

Clinical significance: The value of this study relies on the demonstration that a proper heat-treatment of CAD/CAM lithium disilicate and ZLS glass ceramics generates products that are suitable for clinical use . The differences highlightable in mechanical properties and biocompatibility behavior do not affect their successful clinical application.

1. Introduction

In modern times, the increase of aesthetic perfection request as well as the intense research have led to the development of materials with high capacity of biomimicry [1]. The new materials are, much more than in the past, able to replicate aesthetic-functional characteristics of the

* Corresponding author at: Department of Innovative Technologies in Medicine and Dentistry, University "G. d'Annunzio" of Chieti-Pescara, Via dei Vestini 31, Chieti 66100, Italy.
E-mail address: tonino.traini@unich.it (T. Traini).
[1] These authors contributed equally to this work.

https://doi.org/10.1016/j.jdent.2022.104054
Received 9 November 2021; Received in revised form 31 December 2021; Accepted 31 January 2022
Available online 2 February 2022

teeth. Metal-free restorations, thanks to their increasingly proven clinical efficacy and technological development, have carved out a place of pride for themselves within the current prosthetic treatment plans, becoming a viable alternative to the traditional metal ceramic restorations, both aesthetically and mechanically, in particular for single restorations [2–6].

These new materials include a wide range of glass-ceramics and polycrystalline materials, such as yttria tetragonal zirconia polycrystals (Y-TZP). Y-TZP has excellent mechanical properties, so it finds a wide range of clinical indications [7]. However, it is not without drawbacks, such as its opaque appearance despite the improved aesthetic characteristics [8], and its inertness to the etching procedures for the adhesive application. Emerging evidences confirm that the zirconia adhesive cementation can be successfully achieved if proper operative protocols are respected, though [9,10]. Ceramic chipping and the ageing phenomenon of Low Temperature Degradation (LTD) are further drawbacks [11,12].

Apart from zirconia, the wide diffusion of chairside CAD/CAM systems for whole digital workflow restorations has led to the development of specific dental materials that include a wide range of new nanostructured glass ceramics. Mostly of the new materials are not immediately applicable after the milling procedure, since they must be heat-treated to reach adequate mechanical and aesthetic properties [13]. The lithium disilicate (LS_2), also supported by a remarkable background of clinical experience [14], has proven to be the most widely used material for ceramic restorations by virtue of its great aesthetic appeal. LS_2 restorations, received a broad consensus not only for their aesthetic characteristics and mechanical properties, but also for the excellent workability [13]. Lithium disilicate restorations can be fabricated either with traditional CAD/CAM methods or with ceramic-press methods, unlike zirconia which can only be processed by CAD/CAM methods [13]. CAD lithium disilicate glass ceramic, before the process of crystallization is characterized by an amorphous glassy matrix that, just after the heat treatment for crystallization, becomes a crystalline material with about 70% of crystals of orthorhombic form of lithium disilicate ($Li_2Si_2O_5$). It is to the $Li_2Si_2O_5$ that we must attribute the mechanical and aesthetic properties, and the most important is the high translucency [15]. Recently, a new ceramic material for dental restorations has been introduced. Zirconia reinforced lithium silicate (ZLS) is based on a significant phase of lithium metasilicate (Li_2SiO_3) and a less represented phase of lithium orthophosphate crystals (Li_3PO_4). The glassy matrix is reinforced by around 10% of zirconium dioxide (ZrO_2), which after the final process of crystallization, leads to the formation of a very fine-grained microstructure (Li_2O-ZrO_2-SiO_2). ZLS is marketed in a pre-crystallized or crystallized form. The partially crystallized, to facilitate the CAD/CAM production, is subsequently treated to complete crystallization, getting so the final color and its latest and optimal mechanical properties [16]. The organization of microstructure before and after treatment of crystallization appears to be extremely different, showing the presence within the melt of a multicomponent system due to nucleation process that takes place after heat treatment. From microstructural analyzes, it emerged that it is impossible to highlight zirconia, which is dispersed in the glassy matrix and therefore an integral part in the crystal lattice. The structure described is to be considered, therefore, the main difference compared to materials such as zirconia and the lithium disilicate [17]. Thermal crystallization treatment appears crucial for mechanical and optical properties of the material [18].

For a controlled crystallization of the glass ceramics, without causing deformation and achieve the wished characteristics, a precise heat treatment schedule is provided by manufacturers. Despite this, as the manufacturer's instructions often refer to a specific dental furnace, various problems arise in everyday practice. The different types of existing dental furnaces may bring to an imprecise thermal calibration and undesired final products.

In the present state of knowledge, data regarding the biocompatibility of ZLS materials are scarce and controversial, especially in comparison with CAD LS_2 [16]. No study examines the biocompatibility with human periodontal ligament stem cells (hPDLSCs). In dentistry, hPDLSCs have been the mostly utilized mesenchymal stem cells (MSCs) population. The major advantage of their use for *in vitro* model to assess cell cytocompatibility of different materials consists in their easy isolation and manipulation [19,20].

Therefore, the aims of the present study were to evaluate the crystal growth and the mechanical properties as Vickers hardness (Hv) and fracture toughness (Ft) of LS_2 and two ZLS CAD/CAM glass-ceramics (ZLS VITA Suprinity PC and ZLS Celtra Duo) after heat treatment in a conventional furnace. Biocompatibility through hPDLSCs adhesion was qualitatively assessed, too. The null hypothesis (H0) under test considered no statistically significant differences in Vickers hardness, fracture toughness and crystal dimensions among LS_2, ZLS Suprinity and ZLS Celtra Duo after heat treatment.

2. Materials and methods

To determine the appropriate sample size for the quantitative evaluations, the sample size calculation using Sigma Stat 3.5 (Systat Software, San Jose, CA, USA) was performed. A recent similar work was consulted to set up the *a priori* parameters [21]. About the mechanical tests, to ensure a power of the study (1-β) > 0.80, with an $\alpha = 0.05$, a minimum detectable difference in means of 0,3 and expected standard deviation of 0,2 the study required a group size of 10. About the microstructural analysis, for a 1-β > 0.80, with an $\alpha = 0.05$, a minimum detectable difference in means of 0,3 and expected standard deviation of 0,05 the study required a group size of 2.

2.1. Specimens' preparation

42 parallelepiped shape specimens (3.5 × 3.0 × 1.0 mm) consisting of non-crystallized blocks (Shade A2) for CAD/CAM use were used for the microstructural analysis, the crystallization process, and the mechanical tests.

They were divided into three groups ($n = 14$) according to the material: LS_2 IPS EMax-CAD (Ivoclar Vivadent, Schaan, Liechtenstein) (LS_2), ZLS VITA Suprinity PC (Vita Zahnfabrik, Bad Säckingen, Germany) (ZLSS), ZLS Celtra Duo (Dentsply Sirona, Charlotte, NC, USA) (ZLSC). Crystallization by heat treatment was achieved with a ceramic conventional furnace (Programat EP 510, Ivoclar Vivadent, Schaan, Liechtenstein) using a honeycomb firing tray. Compositions of the glass ceramics used are summarized in Table 1.

Table 1
Manufacturers (in parenthesis) and chemical composition (weight%) of CAD LS_2 and ZLS used in the study.

Chemical component	LS_2 IPS EMax-CAD (Ivoclar Vivadent)	ZLS VITA Suprinity PC(VITA Zahnfabrik)	ZLS Celtra Duo (Dentsply Sirona)
SiO_2	57–80	56–64	58
Li_2O	11–19	15–21	18.5
K_2O	0–13	1–4	
P_2O_5	0–11	3–8	
ZrO_2	0–8	8–12	10.1
ZnO	0–8		
Al_2O_3	0–5	1–4	1.9
MgO	0–5		
La_2O_3		0.1	
Tb_4O_7			1
CeO_2		0–4	2
P_4O_{10}			5
Pigments	0–8	0–6	

SiO_2: silicon dioxide; Li_2O: lithium oxide; K_2O: potassium oxide; P_2O_5: phosphorus pentoxide; ZrO_2: zirconium dioxide; ZnO: zirconium oxide; Al_2O_3: aluminium oxide; MgO: magnesium oxide; La_2O_3: lanthanum oxide; Tb_4O_7: terbium oxide; CeO_2: cerium oxide; P_4O_{10}: phosphorus pentoxide.

The LS_2 specimens were heat treated from 400 to 840 °C, passing through a first step at 770 °C with a holding time of 5 min, and a second phase at 850 °C with a holding time of 7 min. The ZLSS specimens were heat treated starting from 400 °C until to 840 °C with heating rate of 55 °C/min and a holding time of 8 min, while the ZLSC specimens were heat-treated starting from 500 °C until to 820 °C with heat rate of 60 °C/min and a hold time of 2 min. A vacuum was applied twice to LS_2 group, once to ZLSS group, and it was not applied to ZLSC group. Specific data about the thermal treatment (given by the manufacturers) are reported in Table 2.

2.2. Microstructural analysis

For the microstructural analysis and to assay the Vickers hardness and the fracture toughness, the same methods of a previously published work were applied [18]. Six specimens ($n = 2$ per group) were prepared for the microstructural analysis with a slight acidic surface treatment in order to dissolve the vitreous matrix and expose the crystal lattice. The treatment was performed with a hydrofluoric acid solution (1% for 20 s), the specimens were washed with distilled water, the smear was removed in an ultrasonic bath (Puresonic, Kiaccessori, Nola, Italy) in ethyl acetate for 5–10 min and the specimens were stored in ethyl alcohol 96–100% until SEM investigation. Prior to the investigation, the specimens were let completely dry at room temperature, then they were coated with a very thin layer of gold by vacuum sputter using an Emitech K 550 (Emitech, Ashford, Kent, UK). Ten scanning electron microscope (SEM) (Zeiss EVO 50 XVP, Carl Zeiss SMT, Cambridge, UK) images (30,000× and 80,000×) per specimen were used to determine the dimension of crystals. The measure (length of the crystals taken on the maximum diameter) was made using Image-Pro-Plus vers. 6.0 (Media Cybernetics). The software was calibrated for each experimental image using the calibration function. The number of pixels forming the scale bar reported on each digital SEM image was used for linear remapping of the distance in nanometres. The mean and standard deviation were determined considering more than 400 crystals counted.

2.3. Vickers indentation

The specimens were embedded in acrylic resin (Acrylic VLXB, Kemet International, Kent, UK), wet polished up to 1000-grit silicon carbide paper and polishing liquid on a grinding device (TMA2, Grottammare, Italy) to a high-lustre finish and clamped in position before the indentation tests. Fifty indentations were made on each group (five on each specimen, $n = 10$ per group). The indentations were made using a diamond Vickers indenter (angle 136° and area-depth ratio $A = 24.5\ h_c^2$) fixed with the load cell at a universal testing machine (Lloyd 30 K, Lloyd Instruments, Segensworth, UK) under constant load of 50 N for 5 s in a controlled displacement mode at 0.5 mm/sec. To determine the stress intensity, present at the crack tip due to the indentation, the crack tip profile was determined using SEM with LaB6 (Carl Zeiss SMT, Cambridge, UK). The length of radial cracks emanated from each of the four-indented corner sources were measured using Image-Pro-Plus ver. 6.0 (Media Cybernetics, Bethesda, USA). To ensure accuracy, the software was calibrated for each experimental image using a software feature named "Calibration Wizard" which reported the number of pixels between two selected points (scale bar). The linear remapping of the pixel numbers was used to calibrate the distance in μm. Hv was calculated from the standard formula for force divided by contact area:

$$H_v = 1.8544\frac{P}{d^2} \quad (1)$$

where P is the indenter load in N and d is the length of the diagonal in mm.

2.4. Fracture toughness

Fracture toughness of the material was estimated using cracks produced by the hardness indents. It was represented by the term K_{1C} (Mode 1 critical stress intensity factor) and was defined as the critical value of the stress intensity factor at a crack tip necessary to produce catastrophic failure under simple uniaxial loading [22]; the "1″ stands for mode one (uniaxial) and the "C" stands for critical. To determine fracture toughness the Palmqvist equation was used [23]:

$$K_{1C} = \beta_0\left(\frac{P}{l}\right)^{\frac{1}{2}} \quad (2)$$

where P was the applied load, l was the crack length from the tip of the indentation to the crack end, and β_o was an empirical parameter, usually set equal to 7 for a Vickers indenter [23]. Palmqvist cracks were characteristic in that they have an $l^{-0.5}$ dependence. The units of K_{1C} are MPa $m^{1/2}$.

2.5. Differential thermal analysis (DTA)

Three specimens ($n = 1$ per group) were analyzed by heating from room temperature to 1000 °C with a heating rate of 5 °C/min (2 h in total, with a slow cooling), under flowing nitrogen with a Pt/Rh crucible filled with Al_2O_3 (alumina) as reference in a thermoanalyzer (EXSTAR 6000, Seiko Instrument Inc., Tokyo, Japan). DTA was used to determine the crystallization process. An endothermic reaction is an indication of the nucleation process, the melting, or the glass transition (T_g) in the glass, while an exothermic one indicates a crystallization process since the peak height of the exotherm was proportional to the heat evolved during the crystallization.

2.6. Cell culture and specimens' preparation for SEM cellular analysis

For the human periodontal ligament biopsies, the protocol and informed consents came from a previous published work, accepted by Medical Ethics Committee (no. 266/17.04.14), as well as the procedures for cell culture and hPDLSC characterization [24]. The formal consent form was subscribed by all patients prior to sample collection. The Department of Medical, Oral and Biotechnological Sciences and the Laboratory of Stem Cells and Regenerative Medicine are certified in accordance with the quality standard ISO 9001:2015 (certificate no. 32,

Table 2
Parameters of the thermal treatment protocol used for crystallization of the evaluated glass-ceramics.

Material	Initial temperature (°C)	Heating rate 1 (°C/min)	Vacuum 1 (°)	Intermediate temperature (°C)	Holding time (min)	Heating rate 2 (°C/min)	Final temperature (°C)	Vacuum 2 (°C)	Holding time (min)	Cooling (°C)
IPS Emax-CAD	400	60	From 550 to 770	770	5 (in air)	30	840	From 770 to 840	7 (in air)	Up to 700
Suprinity	400	55	From 410 to 840	na	na	na	840	na	8 min	Up to 680
Celtra Duo	500	60	na	na	na	na	820	na	2 min	Up to 750

na = not applicable.

031/15/S).

Five human periodontal ligament biopsies were scraped from human premolar teeth (extracted for orthodontic reasons) of patients in general good health conditions. The tissue was obtained by scaling the roots using Gracey's curettes [25,26]. The specimens were washed five times with phosphate buffered saline (PBS) (LiStarFish) and cultured using TheraPEAK™ MSCGM™ CD BulletKit serum free, chemically defined (MSCGM-CD) medium for the growth of human mesenchymal stem cells (hMSCs) (Lonza, Basel, Switzerland). The medium was changed twice a week, and cells migrating from the explants tissue after reaching about 80% of confluence, were trypsinized (LiStarFish), and after, were sub-cultured until passage 2nd (P2).

Three glass ceramic specimens ($n = 1$ per group) were immersed in absolute ethanol and sterilised with UV-C (200–280 nm) exposure for 30 min on each side inside a laminar flow workstation. Next, they were placed in sterile Petri dishes before cell seeding. They were cultured with hPDLSCs for 21 days and successively were fixed for 4 h at 4 °C in 4% Glutaraldehyde in 0.05 M phosphate buffer (pH 7.4), dehydrated in growing ethanol concentrations, and then critical point dried. They were then mounted on aluminium stubs and sputter gold coated before SEM imaging.

2.7. Statistical analysis

The statistical analyzes were performed using IBM SPSS Statistics (IBM Corp, Armonk, NY, USA). Mean and standard deviation (SD) of crystal dimension, Hv and Ft were obtained. For each variable, the normality and the equality of variance were assessed. The differences in the mean values among the groups were analyzed. In the case of crystals dimensions, the repeated measurements required the application of Repeated Measurements ANOVA. For Hv and Ft, one-way ANOVA was used. In both cases, post hoc Tukey test was applied for multiple comparisons. The threshold to detect statistically significant differences was set at $p < 0.05$.

3. Results

3.1. Microstructure

The microstructure observed in the glass ceramics before the heat treatment for crystallization showed homogeneous fine structure materials with some differences. LS_2 showed a predominant presence of sub-microns platelet-shaped crystal of lithium metasilicate (Li_2SiO_3) and a lesser amount of rounded nanometric crystallites of lithium orthophosphate (Li_2PO_4). ZLSS appeared to be in a nucleated and pre-crystallized microstructure. ZLSC appeared to be in an advanced state

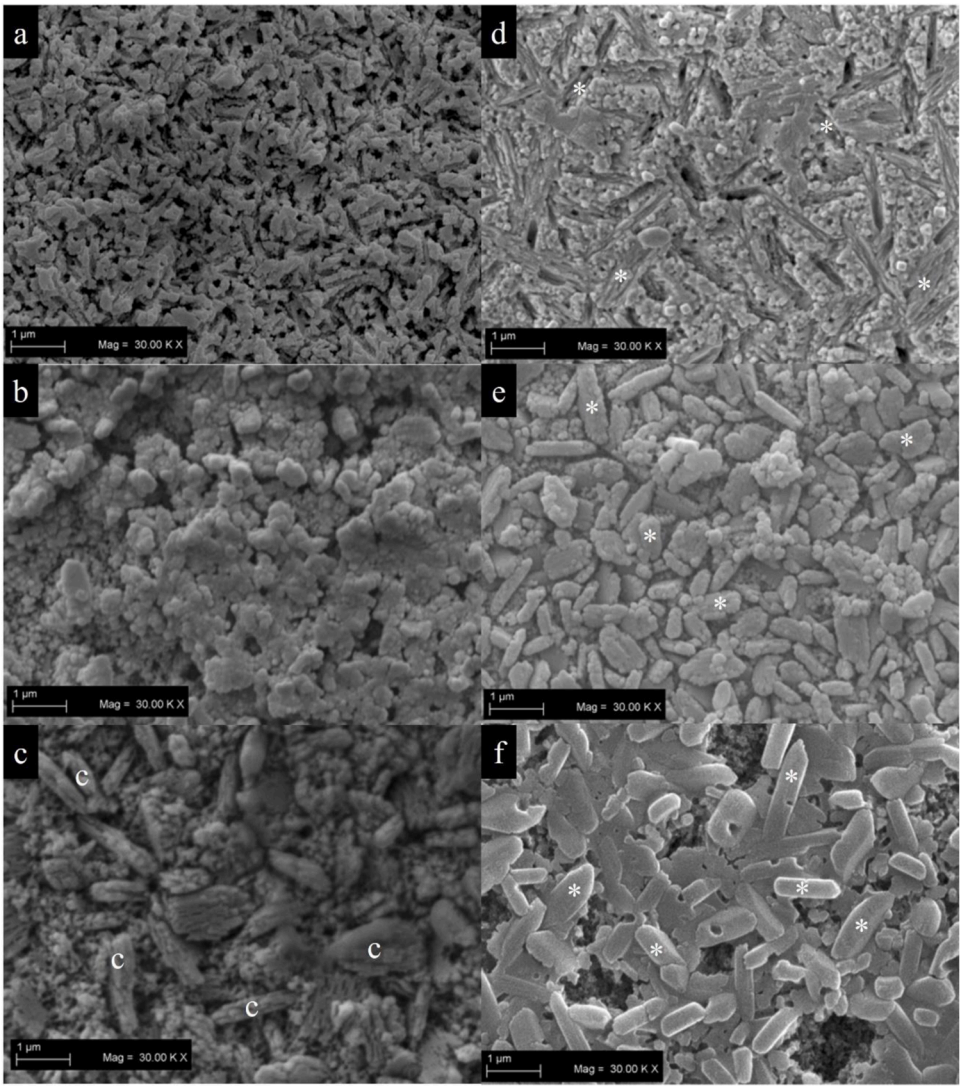

Fig. 1. SEM images of the glass ceramics' microstructure on representative specimens, before and after thermal treatment for crystallization. In (a) LS_2 IPS Emax-CAD (Mag. 30kx), in (b) ZLS Vita Suprinity (Mag. 30kx) and in (c) ZLS Celtra Duo (Mag. 30kx) before thermal treatment. The structure of all groups consists of nanoparticles of homogeneous material immersed in the glassy matrix. ZLSC showed an advanced state of crystallization even before the thermal treatment (c); c: crystallites detectable in ZLSC pre-crystallization state. In (d) LS_2 (Mag. 30kx), in (e) ZLSS (Mag. 30kx) and in (f) ZLSC (Mag. 30kx) after respective thermal treatment. The structures appeared to be changed, with the presence of nanocrystal nucleation and growth into the matrix. LS_2 showed a major extent of the glassy matrix (d); *: representative crystallites. The morphological differences (needle-shaped crystals in LS_2 and globular/rod-like crystals in ZLS) can be noticed both before (more evidently) and after thermal treatment for crystallization.

of crystallization (useful for clinical use) with an almost similar composition of the ZLSS (Fig. 1a–c).

After the crystallization process, LS_2 showed a predominant presence of interlocking needle-shaped crystals of lithium disilicate ($Li_2Si_2O_5$) embedded in a glassy matrix. Both ZLSS and ZLSC showed rounded and road-like crystals of lithium disilicate/metasilicate, lithium monosilicate, aluminium silicate and a glassy matrix enriched with tetragonal zirconia. Basically, LS_2 is featured by needle-shaped crystals, interlocked, and embedded in the glassy matrix, ZLS materials show instead a homogeneous fine crystalline structure with rounded and rod-like crystals, more evident in the post-crystallization state (Fig. 1d–f).

After heat treatment a full crystallized state was obtained, characterized by a crystalline phase with a mean (±SD) crystal size of after heat treatment was 1650.0 (±340.0) nm for LS_2, 854.5 (±155.0) nm for ZLSS and 759.9 (±118.4) nm for ZLSC. Statistically significant differences emerged among the mean values comparisons of all groups ($p < 0.05$) (Fig. 2).

3.2. Vickers hardness

The Hv values (mean ± SD) were 6.1 ± 0.3 GPa for LS_2, 7.6 ± 0.7 GPa for ZLSS and 7.1 ± 0.5 GPa for ZLSC. Statistically significant differences emerged between the mean values of the two ZLS and LS_2 (both with $p < 0.05$), but not between the two ZLSS and ZLSC ($p > 0.05$) (Fig. 3).

3.3. Fracture toughness

The Ft (mean±SD) measured as K_{1C} 2.2 ± 0.1 MPa $m^{1/2}$ for LS_2, 4.7 ± 0.8 MPa $m^{1/2}$ for ZLSS and 3.8 ± 0.6 MPa $m^{1/2}$ for ZLSC. Statistically significant differences of the mean values were detected in all the comparisons among the groups ($p < 0.05$) (Fig. 4).

3.4. Differential thermal analysis

The DTA results are reported in Fig. 5. Specifically, it can be noted a first endothermal event that correspond to the T_g temperature at 580 °C for LS_2, 620 °C for ZLSS and 600 °C for ZLSC. The crystallization process (exothermal peak) for LS_2 occurred at a temperature of 840 °C, for ZLSS at 820 °C and ZLSC at 810 °C.

3.5. Cellular adhesion

Human PDLSCs did not show any significant morphological variations but exhibited different adhesion capability on the three glass ceramic surfaces (Fig. 6a–c). It was possible to note a major amount of cell adherent to LS_2 than on both ZLS surface. The cells preserved their characteristic spindle fibroblast-like shape, although they differently spread upon the surfaces.

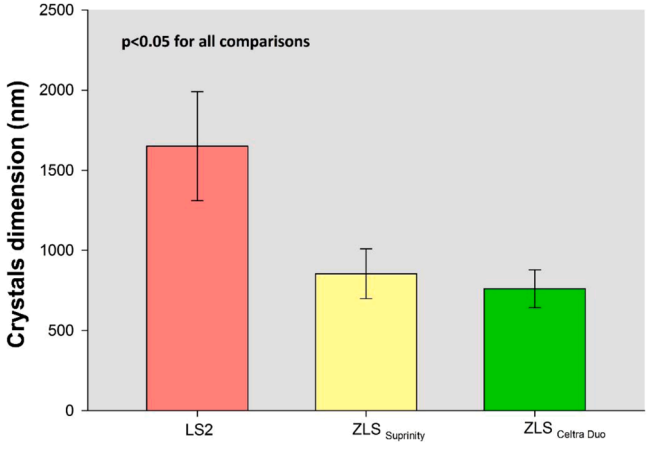

Fig. 2. Representation of crystals dimension (nm) means (±SD) of the three glass ceramics. The differences among the groups were all statistically significant ($p < 0.05$) (RM-ANOVA and Tukey test).

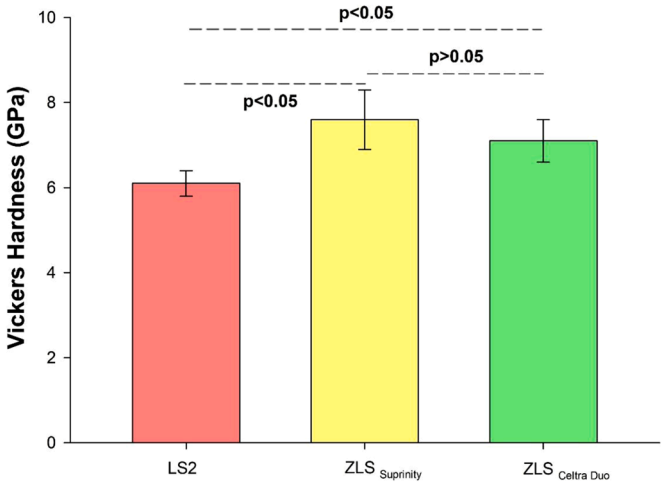

Fig. 3. DTA charts for LS_2 (red), ZLSS (blue) and ZLSC (green). T_g is identified as the endothermal peak at 580 °C, 620 °C and 600 °C, respectively for LS_2, ZLSS and ZLSC. The exothermal peak of crystallization was at 840 °C for LS_2, 820 °C for ZLSS and 810 °C for ZLSC. ΔT: temperature difference (in μw/mg) of the sample with the reference (Al_2O_3) (For interpretation of the references to color in this figure legend, the reader is referred to the web version of this article).

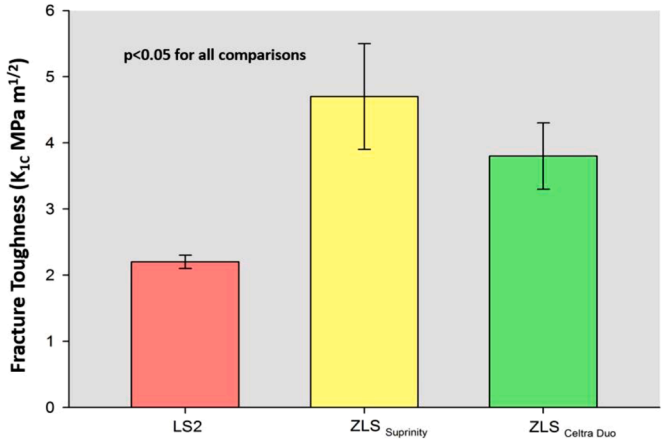

Fig. 4. Representation of Vickers hardness' (GPa) means (±SD) of the three glass ceramics. The differences between LS_2 and the ZLSS and between LS_2 and ZLSC were statistically significant ($p < 0.05$). There was not statistically significant difference between ZLSS and ZLSC ($p > 0.05$) (ANOVA and Tukey test).

4. Discussion

The present investigation mainly aimed to evaluate the influence of the thermal treatment carried out with a conventional furnace on the mechanical properties and the crystal growth of LS_2 and two different ZLS intended for CAD/CAM use. After heat treatment, LS_2 showed statistically significant superior crystal dimension and inferior Vickers hardness and fracture toughness than ZLS Suprinity and ZLS Celtra Duo. The null hypothesis (H_0) was therefore rejected.

Regarding crystals shape and dimensions, it is known that crystallites (mainly lithium metasilicate) in the glassy matrix show different dimensions in ZLSC (about 1 μm) compared to ZLSS (about 0.5 μm) [27, 28], and in both cases smaller than LS_2 crystals, with length comprised between 0.5 and 4 μm [29]. In the present study, it was confirmed that

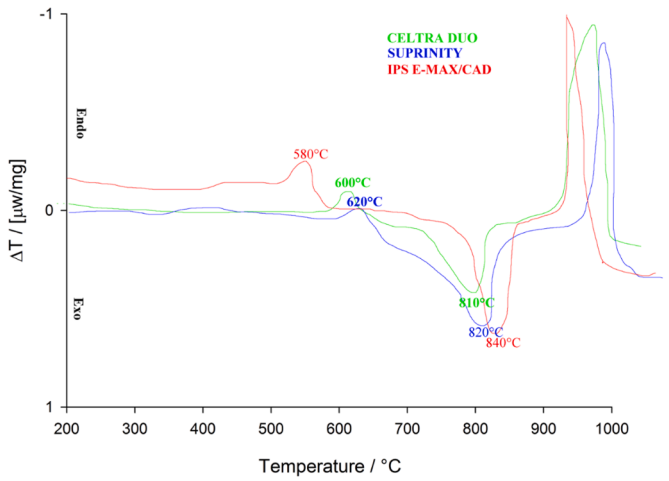

Fig. 5. Representation of fracture toughness (K_{1C}) (MPa $m^{1/2}$) means (±SD) of the three glass ceramics. The differences among the groups were all statistically significant ($p < 0.05$) (ANOVA and Tukey test).

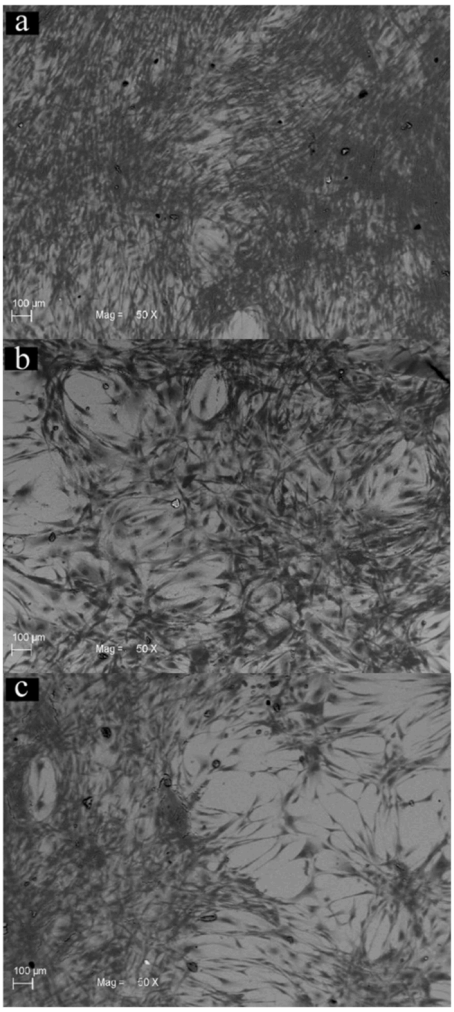

Fig. 6. SEM images (Mag. 50x) of hPDLSCs culture on the three glass ceramics: (a) LS2; (b) ZLSS; (c) ZLSC. The spindle fibroblast-like shape of the cultured cells was preserved, but a major number of adherent cells can be noted on LS_2 with respect to ZLS ceramics. The more represented glassy matrix of LS_2 can influence the cellular adhesion.

ZLS crystals are smaller than LS_2 ones. It has to be noted that the LS_2 crystals dimension here was 1650.0 (±340.0) nm, so in agreement with the literature data, but for ZLSS (854.5 ± 155.0 nm) and for ZLSC (759.9 ± 118.4 nm) crystals dimensions were inferior to the data reported in literature. In addition, statistical differences were detected not only in ZLSS and ZLSC vs LS_2, but also between ZLSS and ZLSC (Fig. 2). A reason for this discrepancy can likely be the different methods of analysis used, and the furnace used for the thermal treatment. Here it was a conventional furnace, and in the previous studies the dedicated one.

To date, there are controversial data on the mechanical properties of ZLS. It must be considered that this issue may be attributed to the multiplicity of *in vitro* research designs and testing modalities. The comparisons are therefore difficult, as well as the possible correlations with the biomechanical attitude *in vivo*. Here, the Hv of the two ZLS were significantly superior to LS_2, but (even if ZLSS Hv was the highest one, 7.6 ± 0.7 GPa) no differences between the two ZLS were found (Fig. 4). On the contrary, significant differences among all groups were found regarding Ft, with ZLSS showing the highest value (4.7 ± 0.8 MPa $m^{1/2}$) (Fig. 5). The collected data demonstrated that ZLS exhibits superior mechanical properties compared to lithium-disilicate glass ceramics. The indentation cracking method used is suitable to determine the surface fracture toughness of hard brittle materials because it is easy to perform, while causing negligible surface damage [30,31]. Fracture toughness (K_{1C}) represents the intrinsic properties of a material to resist crack propagation under an applied load, and it is a parameter usually applied to a homogeneous, linear elastic material and is useful for providing a failure criterion for brittle materials [32]. It is a measure of the maximum energy a material could absorb before fracture takes place [33]. Fracture occurs when the intensity of the stress field reaches this threshold. Fracture toughness strongly depends on composition and the microstructure of the material: the crack-microstructure interactions can affect crack propagation and hence the fracture toughness [34]. Interestingly, Sieper et al. [35] found that in ZLS the presence of semi-circular arrest lines close to the origin of failure constitutes an effective mechanism of crack interruption. The crack formation and propagation might be hindered by the transformation of the tetragonal zirconia phase. In fact, in ZLS zirconia fillers are the responsible for this additional toughening mechanism, determining its superior Ft [36]. This issue has been questioned by some authors, though [29].

The presented findings show that the finer grained structure of ZLS with respect to LS_2 clearly has an impact on the resistance to permanent deformation (Hv) and on the ability of containing a crack to resist further fracture (Ft). It can be speculated that the difference in crystal dimension and Ft between ZLSS and the ZLSC, but not in Hv, can be caused by the difference in their chemical composition, in their crystallization thermal treatment or even by their industrial production process. It is interesting to note that ZLSS showed higher values of Ft even with a significant superior mean crystals dimension than ZLSC, suggesting that the crystals dimension may not be the paramount parameter influencing Ft. Further studies are needed to address this issue. Notwithstanding this, it has to be noticed that the Ft of the dental enamel was reported as ranging between 0.7 ± 0.2 MPa $m^{1/2}$ and 1.77±0.2 MPa $m^{1/2}$ while, the Hv values showed 4.7 ± 0.3 GPa [37], therefore all the tested materials can be suitable for clinical application, also in the molar area, where the masticatory load can even reach 600–900 N in case of severe bruxism [38].

DTA analysis was performed to identify the transformation temperatures for each type of material considered in the present study (Fig. 3). The T_g of the different materials was highlighted at a range temperature 580–620 °C. It reflects the kinetic transition mainly attributable to the glassy phase of the material. The crystallization process is an exothermal process instead, that exhibit typical peaks in the DTA evaluations for glass ceramics. Exothermal peaks occurred between 810–840 °C. All the curves reveal sharp peaks in the respective temperature interval, indicating an internal, bulk crystallization, since sharp peaks implies bulk crystallization while a broad peak signifies surface crystallization [39].

Typically, the shape of a DTA peak depends on specimen's weight and the heating rate used. Here it was chosen to apply a slow heating rate, since lowering the heating rate is roughly equivalent to reducing specimen weight, both lead to sharper peaks with improved resolution. The influence of heating rate on the peak shape and disposition can be used to advantage in the study of decomposition reactions, but for kinetic analysis, as crystallization, it is important to minimise thermal gradients by reducing specimen size or heating rate [40].

SEM analysis showed that cell adhesion was superior on LS_2 specimens compared to ZLS ones, with a pristine morphological appearance of hPDLSC in all cases. The major content of the glass phase in the LS_2 structure can be the factor determining this superior cellular adhesion. This indicates that entirely crystallized and polished CAD LS_2 provides more favourable tissues' response than ZLS. As reported by a recent literature review [16], only one recent study quantitatively compare biocompatibility of ZLS and CAD LS_2 [41]. The findings herein qualitatively presented agree with those of the cited study, even if the authors evaluate biocompatibility studying cell viability and collagen secretion using human gingival fibroblasts, rather than cellular adhesion parameters. It is clear that also in the cytocompatibility field, data about ZLS are scares and heterogeneous, considering the newness of the material, as well as, surprisingly, CAD LS_2. There is a need for further research to shed more light on this theme.

The main limitation of this study is not to have a clinical counterpart to match the results with, to obtain a thorough comprehension of the studied glass ceramics' performance and biological response. Data reported by *in vitro* studies should be further corroborated by *in vivo* results of clinical, long-term survival rates. Nevertheless, the important finding that optimal chemical and mechanical properties can be achieved even processing these materials with conventional furnaces if the given thermal treatment protocol is respected, is of worth.

5. Conclusion

The results of this study demonstrated that:

(1) CAD/CAM lithium disilicate and ZLS glass ceramics showed a crystallization process highly dependant to temperature.
(2) After crystallization treatment, ZLS glass ceramics show significantly inferior crystals dimensions and higher fracture toughness and Vickers hardness than LS_2. Differences in crystals dimension and fracture toughness exist between ZLS Suprinity and ZLS Celtra Duo as well.
(3) Respecting the manufacturers' thermal treatment schedule, it is possible to achieve adequate chemical and mechanical properties of CAD/CAM lithium disilicate and ZLS glass ceramics.
(4) *In vitro* qualitative analysis showed that human periodontal ligament stem cells better adhere onto CAD/CAM lithium disilicate than onto ZLS surfaces.
(5) Notwithstanding the above, the differences highlighted among the materials are compatible with their successful application in the clinical scenario.

Ethics statement

The biocompatibility study was approved by the Ethics Committee Medical School, "G. d'Annunzio" University, Chieti, Italy (protocol no. 266/17.04.14).

Funding

This research was funded by Prof. Tonino Traini ex 60% University of Chieti funds.

CRediT authorship contribution statement

Luan Mavriqi: Methodology, Investigation, Writing – review & editing. **Francesco Valente:** Methodology, Investigation, Visualization, Writing – original draft. **Giovanna Murmura:** Data curation, Supervision. **Bruna Sinjari:** Validation, Formal analysis, Writing – review & editing. **Monica Macrì:** Data curation, Supervision, Writing – review & editing. **Oriana Trubiani:** Conceptualization, Investigation, Supervision, Project administration. **Sergio Caputi:** Validation, Supervision, Project administration. **Tonino Traini:** Conceptualization, Investigation, Data curation, Formal analysis, Writing – review & editing.

Declaration of Competing Interest

The authors declare that they have no competing financial interests.

Bibliography

[1] A. Vichi, C. Louca, G. Corciolani, M. Ferrari, Color related to ceramic and zirconia restorations: a review, Dent. Mater. 27 (2011) 97–108, https://doi.org/10.1016/j.dental.2010.10.018.
[2] F. Zarone, S. Russo, R. Sorrentino, From porcelain-fused-to-metal to zirconia: clinical and experimental considerations, Dent. Mater. 27 (2011) 83–96, https://doi.org/10.1016/j.dental.2010.10.024.
[3] I. Sailer, A. Fehér, F. Filser, L.J. Gauckler, H. Lüthy, C.H.F. Hämmerle, Five-year clinical results of zirconia frameworks for posterior fixed partial dentures, Int. J. Prosthodont. 20 (2007) 383–388.
[4] P.C. Guess, S. Schultheis, E.A. Bonfante, P.G. Coelho, J.L. Ferencz, N.R.F.A. Silva, All-ceramic systems: laboratory and clinical performance, Dent. Clin. N. Am. 55 (2011) 333–352, https://doi.org/10.1016/j.cden.2011.01.005, ix.
[5] I. Sailer, N.A. Makarov, D.S. Thoma, M. Zwahlen, B.E. Pjetursson, All-ceramic or metal-ceramic tooth-supported fixed dental prostheses (FDPs)? A systematic review of the survival and complication rates. Part I: single crowns (SCs), Dent. Mater. 31 (2015) 603–623, https://doi.org/10.1016/j.dental.2015.02.011.
[6] B.E. Pjetursson, I. Sailer, N.A. Makarov, M. Zwahlen, D.S. Thoma, All-ceramic or metal-ceramic tooth-supported fixed dental prostheses (FDPs)? A systematic review of the survival and complication rates. Part II: multiple-unit FDPs, Dent. Mater. 31 (2015) 624–639, https://doi.org/10.1016/j.dental.2015.02.013.
[7] T. Miyazaki, T. Nakamura, H. Matsumura, S. Ban, T. Kobayashi, Current status of zirconia restoration, J. Prosthodont. Res. 57 (2013) 236–261, https://doi.org/10.1016/j.jpor.2013.09.001.
[8] Y. Zhang, Making yttria-stabilized tetragonal zirconia translucent, Dent. Mater. 30 (2014) 1195–1203, https://doi.org/10.1016/j.dental.2014.08.375.
[9] F. Valente, L. Mavriqi, T. Traini, Effects of 10-MDP based primer on shear bond strength between zirconia and new experimental resin cement, Materials 13 (2020) E235, https://doi.org/10.3390/ma13010235 (Basel).
[10] X. Yue, X. Hou, J. Gao, P. Bao, J. Shen, Effects of MDP-based primers on shear bond strength between resin cement and zirconia, Exp. Ther. Med. 17 (2019) 3564–3572, https://doi.org/10.3892/etm.2019.7382.
[11] C. Larsson, A. Wennerberg, The clinical success of zirconia-based crowns: a systematic review, Int. J. Prosthodont. 27 (2014) 33–43, https://doi.org/10.11607/ijp.3647.
[12] T. Sato, M. Shimada, Transformation of yttria-doped tetragonal ZrO_2 polycrystals by annealing in water, J. Am. Ceram. Soc. 68 (1985) 356, https://doi.org/10.1111/j.1151-2916.1985.tb15239.x. –356.
[13] F. Zarone, M.I. Di Mauro, P. Ausiello, G. Ruggiero, R. Sorrentino, Current status on lithium disilicate and zirconia: a narrative review, BMC Oral Health 19 (2019) 134, https://doi.org/10.1186/s12903-019-0838-x.
[14] L. Mavriqi, F. Valente, B. Sinjari, O. Trubiani, S. Caputi, T. Traini, Water-airborne-particle abrasion as a pre-treatment to improve bioadhesion and bond strength of glass-ceramic restorations: from *in vitro* study to 15-year survival rate, Materials 14 (2021) 4966, https://doi.org/10.3390/ma14174966 (Basel).
[15] A. Willard, T.M. Gabriel Chu, The science and application of IPS e. Max dental ceramic, Kaohsiung J. Med. Sci. 34 (2018) 238–242, https://doi.org/10.1016/j.kjms.2018.01.012.
[16] F. Zarone, G. Ruggiero, R. Leone, L. Breschi, S. Leuci, R. Sorrentino, Zirconia-reinforced lithium silicate (ZLS) mechanical and biological properties: a literature review, J. Dent. 109 (2021), 103661, https://doi.org/10.1016/j.jdent.2021.103661.
[17] S. Krüger, J. Deubener, C. Ritzberger, W. Höland, Nucleation kinetics of lithium metasilicate in ZrO_2-bearing lithium disilicate glasses for dental application, Int. J. Appl. Glass Sci. 4 (2013) 9–19, https://doi.org/10.1111/ijag.12011.
[18] T. Traini, B. Sinjari, R. Pascetta, N. Serafini, G. Perfetti, P. Trisi, S. Caputi, The zirconia-reinforced lithium silicate ceramic: lights and shadows of a new material, Dent. Mater. J. 35 (2016) 748–755, https://doi.org/10.4012/dmj.2016-041.
[19] F. Diomede, I. Merciaro, S. Martinotti, M.F.X.B. Cavalcanti, S. Caputi, E. Mazzon, O. Trubiani, miR-2861 is involved in osteogenic commitment of human periodontal ligament stem cells grown onto 3D scaffold, J. Biol. Regul. Homeost. Agents 30 (2016) 1009–1018.
[20] J. Pizzicannella, F. Diomede, A. Gugliandolo, L. Chiricosta, P. Bramanti, I. Merciaro, T. Orsini, E. Mazzon, O. Trubiani, 3D printing PLA/Gingival stem

cells/EVs upregulate miR-2861 and -210 during osteoangiogenesis commitment, Int. J. Mol. Sci. 20 (2019) 3256, https://doi.org/10.3390/ijms20133256.
[21] A. Ozdogan, Z. Yesil Duymus, Investigating the effect of different surface treatments on vickers hardness and flexural strength of zirconium and lithium disilicate ceramics, J. Prosthodont. 29 (2020) 129–135, https://doi.org/10.1111/jopr.12939.
[22] J.F. Shackelford, Introduction to Materials Science For Engineers, 8th ed., Pearson, Boston, 2015.
[23] B. Roebuck, E. Bennett, L. Lay, R. Morrell, Palmqvist Toughness for Hard and Brittle Materials, National Physical Laboratory, 2008.
[24] G.D. Marconi, F. Diomede, J. Pizzicannella, L. Fonticoli, I. Merciaro, S. D. Pierdomenico, E. Mazzon, A. Piattelli, O. Trubiani, Enhanced VEGF/VEGF-R and RUNX2 expression in human periodontal ligament stem cells cultured on sandblasted/etched titanium disk, Front. Cell Dev. Biol. 8 (2020) 315, https://doi.org/10.3389/fcell.2020.00315.
[25] O. Trubiani, P. Ballerini, G. Murmura, J. Pizzicannella, P. Giuliani, S. Buccella, S. Caputi, Toll-like receptor 4 expression, interleukin-6, -8 and Ccl-20 Release, and NF-KB translocation in human periodontal ligament mesenchymal stem cells stimulated with LPS-P. Gingivalis, Eur. J. Inflamm. 10 (2012) 81–89, https://doi.org/10.1177/1721727X1201000109.
[26] F. Diomede, M. D'Aurora, A. Gugliandolo, I. Merciaro, T. Orsini, V. Gatta, A. Piattelli, O. Trubiani, E. Mazzon, Biofunctionalized scaffold in bone tissue repair, Int. J. Mol. Sci. 19 (2018) 1022, https://doi.org/10.3390/ijms19041022.
[27] R. Belli, M. Wendler, D. de Ligny, M.R. Cicconi, A. Petschelt, H. Peterlik, U. Lohbauer, Chairside CAD/CAM materials. Part 1: measurement of elastic constants and microstructural characterization, Dent. Mater. 33 (2017) 84–98, https://doi.org/10.1016/j.dental.2016.10.009.
[28] M. Wendler, R. Belli, A. Petschelt, D. Mevec, W. Harrer, T. Lube, R. Danzer, U. Lohbauer, Chairside CAD/CAM materials. Part 2: flexural strength testing, Dent. Mater. 33 (2017) 99–109, https://doi.org/10.1016/j.dental.2016.10.008.
[29] N.de C. Ramos, T.M.B. Campos, I.S. de L. Paz, J.P.B. Machado, M.A. Bottino, P. F. Cesar, R.M. de Melo, Microstructure characterization and SCG of newly engineered dental ceramics, Dent. Mater. 32 (2016) 870–878, https://doi.org/10.1016/j.dental.2016.03.018.
[30] K.J. Soderholm, Review of the fracture toughness approach, Dent. Mater. 26 (2010) e63–e77, https://doi.org/10.1016/j.dental.2009.11.151.
[31] A. Leonardi, F. Furgiuele, S. Syngellakis, R.J.K. Wood, Analytical approaches to stress intensity factor evaluation for indentation cracks, J. Am. Ceram. Soc. 92 (2009) 1093–1097, https://doi.org/10.1111/j.1551-2916.2009.03070.x.
[32] W. Oh, N.Z. Zhang, K.J. Anusavice, Effect of heat treatment on fracture toughness (KIC) and microstructure of a fluorcanasite-based glass-ceramic, J. Prosthodont. 16 (2007) 439–444, https://doi.org/10.1111/j.1532-849X.2007.00233.x.
[33] M. Bhat, B. Kaur, R. Kumar, K.K. Bamzai, P.N. Kotru, B.M. Wanklyn, Effect of ion irradiation on dielectric and mechanical characteristics of $ErFeO_3$ single crystals, Nucl. Inst. Methods Phys. Res. B 4 (2005) 494–508, https://doi.org/10.1016/j.nimb.2005.01.119.
[34] J.B. Quinn, V. Sundar, I.K. Lloyd, Influence of microstructure and chemistry on the fracture toughness of dental ceramics, Dent. Mater. 19 (2003) 603–611, https://doi.org/10.1016/s0109-5641(03)00002-2.
[35] K. Sieper, S. Wille, M. Kern, Fracture strength of lithium disilicate crowns compared to polymer-infiltrated ceramic-network and zirconia reinforced lithium silicate crowns, J. Mech. Behav. Biomed. Mater. 74 (2017) 342–348, https://doi.org/10.1016/j.jmbbm.2017.06.025.
[36] R. Badawy, O. El-Mowafy, L.E. Tam, Fracture toughness of chairside CAD/CAM materials – alternative loading approach for compact tension test, Dent. Mater. 32 (2016) 847–852, https://doi.org/10.1016/j.dental.2016.03.003.
[37] M.Á. Garrido, I. Giráldez, L. Ceballos, J. Rodríguez, On the possibility of estimating the fracture toughness of enamel, Dent. Mater. 30 (2014) 1224–1233, https://doi.org/10.1016/j.dental.2014.08.364.
[38] A. Waltimo, M. Nyström, M. Känänen, Bite force and dentofacial morphology in men with severe dental attrition,, Eur. J. Oral Sci. 102 (1994) 92–96, https://doi.org/10.1111/j.1600-0722.1994.tb01161.x.
[39] J.A. Augis, J.E. Bennett, Calculation of the Avrami parameters for heterogeneous solid state reactions using a modification of the Kissinger method, J. Therm. Anal. 13 (1978) 283–292, https://doi.org/10.1007/BF01912301.
[40] N. Monmaturapoj, P. Lawita, W. Thepsuwan, Characterisation and properties of lithium disilicate glass ceramics in the SiO_2 -Li_2O-K_2O-Al_2O_3 system for dental applications, Adv. Mater. Sci. Eng. 2013 (2013) 1–11, https://doi.org/10.1155/2013/763838.
[41] M. Rizo-Gorrita, C. Herráez-Galindo, D. Torres-Lagares, M.Á. Serrera-Figallo, J. L. Gutiérre-Pérez, Biocompatibility of polymer and ceramic CAD/CAM materials with human gingival fibroblasts (HGFs), Polymers 11 (2019) 1446, https://doi.org/10.3390/polym11091446 (Basel).